Discrete contribution to $\psi' \rightarrow J/\psi + \gamma\gamma$

Zhi-Guo He,[1,*] Xiao-Rui Lu,[2,†] Joan Soto,[1,‡] and Yangheng Zheng[2,§]

[1]*Departament d'Estructura i Constituents de la Matèria and Institut de Ciències del Cosmos,*
Universitat de Barcelona, Diagonal, 647, E-08028 Barcelona, Catalonia, Spain
[2]*Physics Department, Graduate University of Chinese Academy of Sciences, Beijing, 100049, China*

The decay mode $\psi(2S) \rightarrow J/\psi + \gamma\gamma$ is proposed in order to experimentally identify the effects of the coupling of charmonium states to the continuum $D\bar{D}$ states. To have a better understanding of such a two-photon decay process, in this work we restrict ourselves to investigate the contribution of the discrete part, in which the photons are mainly produced via the intermediate states $\chi_{cJ}(nP)$. Besides calculating the resonance contributions of $\chi_{cJ}(1P)(J = 0, 1, 2)$, we also take into account the contributions of the higher excited states $\chi_{cJ}(2P)$ and the interference effect among the $1P$ and $2P$ states. We find that the contribution of the $2P$ states and the interference terms to the total decay width is very tiny. However, for specific regions of the Dalitz plot, off the resonance peaks, we find that these contributions are sizable and should also be accounted for. We also provide the photon spectrum and study the polarization of J/ψ.

I. INTRODUCTION

Electromagnetic processes have always provided invaluable probes of the strong interactions, the most prominent example being the deep inelastic scattering experiments in the early 1970s which eventually established QCD as the fundamental theory of the strong interactions. Among the current challenges of QCD is the description of the plethora of charmoniumlike states discovered during the past years, the so-called "XYZ" (for reviews see, e.g., Refs. [1–4]), that lie above the $D\bar{D}$ threshold, and do not fit potential model expectations. It is widely accepted that the effects of the coupling of a core charmonium, namely, a mainly $c\bar{c}$ bound state, to a $D\bar{D}$ meson pair, the so-called coupled-channel effects, are an important ingredient to understand those states. We shall call the latter continuum states and the former valence states. We will argue below that two-photon transitions between heavy quarkonium states may provide important experimental information on the continuum-valence coupling.

Historically, it has been recognized for a long time that the continuum states may shift the mass spectrum of a pure $c\bar{c}$ state considerably [5–7]. Recently, exploratory investigations on the mixing between discrete and continuum states in charmonium have been carried out in lattice QCD [8]. Lattice QCD has also provided a detailed study of the so-called "string breaking" in the static approximation [9], which may be used to extract information on the continuum-valence coupling [10]. If the heavy quark mass m is much larger than the remaining scales in the system, then the heavy quarks move slowly in their center-of-mass frame, say with a typical velocity $v_Q \ll 1$, that is,

with typical three momentum mv_Q and hence with typical binding energy mv_Q^2. Nonrelativistic QCD (NRQCD) [11–13] can be used to factorize the contributions from energies larger or of the order of m, and provides a good starting point. Recall that the heavy-light meson pair threshold lies at a typical nonrelativistic energy $\sim \Lambda_{QCD}$, according to heavy quark effective theory (HQET) counting rules [14]. Then, if the binding energy of a heavy quarkonium state lies much below open flavor threshold, namely, $mv_Q^2 \ll \Lambda_{QCD}$ one can integrate out energies of order $\sim \Lambda_{QCD}$. This leads to potential NRQCD (pNRQCD) in the strong coupling regime [15]. The dynamics of this effective theory reduces to a heavy quark and a heavy antiquark interacting through a potential [16–18] (see [19] for a review). Hence, in order to understand the properties of these states, there is no need to introduce explicitly the continuum states if the potential is chosen appropriately. However, for states close to or above the open flavor threshold, the coupling of continuum to valence states needs to be addressed, and so far it is not known how to proceed in a model independent way.[1] Hence, most of the analysis has been done by using different models. Recently, some general features of the coupled-channel effects have been obtained in the quark model [22] under the assumptions that valence-continuum coupling is described by the $^3P_0$ model [23] and the interaction between two mesons is negligible. These results suggest that for the low-lying states the effect of continuum channels is hidden in the parameters in the potential model. In Ref. [24], it is mentioned that the radiative transition process may be sensitive to the continuum components.

---

*hzgzlh@ecm.ub.es
†xiaorui@gucas.ac.cn
‡joan.soto@ub.edu
§zhengyh@gucas.ac.cn

[1]A hadronic effective theory has recently been introduced to study particular states very close to threshold, most notably the $X(3872)$, which includes coupled-channel effects [20]. See also [21] for an even more recent proposal.

However, previous works, based on Cornell coupled-channel formalism, indicate that the relativistic corrections [25,26] may be more important than the continuum contributions [27]. Therefore, it is not straightforward to disentangle the continuum contributions in the one-photon transition process.

Here, we propose a new process, namely, $\psi(2S) \rightarrow J/\psi + \gamma\gamma$ which can provide an additional opportunity to pin down the valence-continuum coupling. From the theoretical point of view, electromagnetic transitions allow a cleaner analysis than hadronic decay processes. At the amplitude level, the contribution to this two-photon transition can be divided into two parts. We refer to the first one as the discrete part, which involves charmonium states only. The discrete part is dominated by the following process: the $\psi(2S)$ state decays into a real or virtual $\chi_{cJ}(nP)$ state by radiating one photon, and then, the real or virtual $\chi_{cJ}(nP)$ state decays into J/ψ plus another photon. This process not only includes the cascade decay process (on-shell region), but also the off-shell region. We will study the whole phase space. The second part is referred to as the continuum part, in which at least one photon is emitted by an intermediate charmed meson. In the discrete part, the $\chi_{cJ}(1P)(J = 0, 1, 2)$ states can be on-shell, so the total contribution of the discrete subprocess should be much larger than that of the continuum part. However, when the invariant mass of J/ψ and one of the photons is far away from the resonance regions of the $\chi_{cJ}(1P)(J = 0, 1, 2)$ states, the discrete part contribution will drop down very fast. Thus, the contribution of the continuum part may be important and measurable in the off-shell region. Let us mention that in Ref. [28], a similar decay process of $B(D)^* \rightarrow B(D) + 2\gamma$ is suggested to determine the values of the strong couplings $g_{B(D)^*B(D)\pi}$ and $g_{B(D)^*B(D)\gamma}$.

On the experimental side, such a two-photon transition process has already been studied in the 1970s and 1980s [29,30]. In recent years, more precise measurements were carried out by the BESIII [31,32] and CLEO [33,34] Collaborations. However, they focused on the investigation of the cascade decay $\psi(2S) \rightarrow \chi_{cJ} + \gamma$ followed by $\chi_{cJ} \rightarrow J/\psi + \gamma$ and on the study of the properties of the χ_{cJ} states. Only in Ref. [34], was a discussion made on the possible amplitude of the two-photon transition in treating the backgrounds of the χ_{cJ} states. Hence, so far, no one has ever used it to study coupled-channel effects. Recently, the BESIII [35] Collaboration reported the significant data excess from the known cascade backgrounds, which was interpreted as the nonresonance decay of $\psi(2S) \rightarrow J/\psi\gamma\gamma$. We remark that this measurement is very sensitive to the line shapes of the χ_{cJ} states, especially in the data selection region.

Because of the above reason, the significance of an eventual experimental determination of the continuous process depends very much on our knowledge on the discrete states. As far as we know, the discrete contribution has not been fully studied yet, and only the individual contribution of each χ_{cJ} state is known by using the nonrelativistic Breit-Wigner formula together with the dynamical factors to describe the χ_{cJ} line shape in the cascade decay of $\psi(2S) \rightarrow \chi_{cJ} + \gamma$ and $\chi_{cJ} \rightarrow J/\psi + \gamma$ [34]. So, in this paper we restrict ourselves to analyze the discrete contribution to this decay assuming that the coupling of ψ' and J/ψ to $D\bar{D}$ is zero, and leave for a future work, the detailed evaluation of $D\bar{D}$ meson pair loops effects.

In this work, we will use effective field theory methods to calculate the decay width, the photon spectrum, and the J/ψ polarization in the discrete subprocess. A complete study of the whole contribution of the discrete $\chi_{cJ}(1P)$ states together with some higher radial excitations, $\chi_{cJ}(2P)$,[2] will be carried out. The rest of this paper is organized as followings: in Sec. II, we will briefly introduce the effective Lagrangian we use and determine the value of the effective couplings; in Sec. III, we will calculate the discrete contribution to the $\psi(2S) \rightarrow J/\psi + \gamma\gamma$ process and show the results, and the discussion and summary will be given in the last section.

II. EFFECTIVE LAGRANGIAN FOR RADIATIVE TRANSITIONS

The heavy quarkonium states are mainly constituted by a $Q\bar{Q}$ pair and classified according to the spectroscopic notation $n^{2S+1}L_J$, where $n = 1, 2, \ldots$ is the radial quantum number, $S = 0, 1$ is the total spin of the heavy quark pair, $L = 0, 1, 2 \ldots$ (or $S, P, D \ldots$) is the orbital angular momentum, and J is the total angular momentum. They have parity $P = (-1)^{L+1}$ and charge conjugation $C = (-1)^{L+S}$.

As mentioned in the introduction, NRQCD is a good starting point to describe this system. The LO NRQCD Lagrangian is invariant under $S = SU(2)_Q \otimes SU(2)_{\bar{Q}}$ spin-symmetry group, an approximate symmetry of the heavy quarkonium states, that is inherited in the subsequent effective theories. We assume that the entire dynamics of these states can be described by a (nonperturbative) potential. That is the case if they are in the strong coupling regime of pNRQCD. This is a reasonable assumption for the $\chi_{cJ}(1P)$ states [36], and to lesser extend for J/ψ.[3] The remaining states are close to or above threshold and are subject to the uncertainties due to the influence of $D\bar{D}$ pairs, that we plan to analyze in a separate work. In any case, we will only use the fact that the typical energy of the emitted photons is at the ultrasoft

---

[2]The contribution of higher nP states, where $n \geq 3$, are ignored.

[3]There are indications that J/ψ may well be better described by the weak coupling regime of pNRQCD [37–39]. At leading order in this regime, the dynamics is described by a (perturbative) potential, and the multipole expansion also holds.

scale mv_Q^2, and the typical size of the system at the soft scale $\frac{1}{mv_Q}$. This allows us to carry out the multipole expansion of the photon field about the center-of-mass coordinate, which means that the photons see the heavy quarkonium states as pointlike particles. Hence, it is most convenient to introduce hadronic spin-symmetry multiplets, in an analogous way as it was initially done in HQET [14].

For heavy quarkonium states, this formalism was developed in Ref. [40]. The states have the same radial number n and the same orbital momentum L can also be expressed by means of a single multiplet $J^{\mu_1\cdots\mu_L}$ [40],

$$
\begin{aligned}
J^{\mu_1\cdots\mu_L} = \frac{1+\not{v}}{2}\Bigg(& H_{L+1}^{\mu_1\cdots\mu_L\alpha}\gamma_\alpha + \frac{1}{\sqrt{L(L+1)}}\sum_{i=1}^{L}\epsilon^{\mu_i\alpha\beta\gamma}v_\alpha\gamma_\beta H_{L\gamma}^{\mu_1\cdots\mu_{i-1}\mu_{i+1}\cdots\mu_L} \\
& + \frac{1}{L}\sqrt{\frac{2L-1}{2L+1}}\sum_{i=1}^{L}(\gamma^{\mu_i}-v^{\mu_i})H_{L-1}^{\mu_1\cdots\mu_{i-1}\mu_{i+1}\cdots\mu_L} - \frac{2}{L\sqrt{(2L-1)(2L+1)}} \\
& \times \sum_{i<j}(g^{\mu_i\mu_j}-v^{\mu_i}v^{\mu_j})\gamma_\alpha H_{L-1}^{\alpha\mu_1\cdots\mu_{i-1}\mu_{i+1}\cdots\mu_{j-1}\mu_{j+1}\cdots\mu_L} + K_L^{\mu_1\cdots\mu_L}\gamma^5\Bigg)\frac{1-\not{v}}{2},
\end{aligned} \tag{1}
$$

where v^μ is the four velocity associated to the multiplet $J^{\mu_1\cdots\mu_L}$ (not to be mistaken by v_Q, the typical velocity of the heavy quark in the heavy quarkonium rest frame), $K_L^{\mu_1\cdots\mu_L}$ represents the spin-singlet effective field, and $H_{L-1}^{\mu_1\cdots\mu_{L-1}}, H_L^{\mu_1\cdots\mu_L}$ and $H_{L+1}^{\mu_1\cdots\mu_{L+1}}$ represent the three spin-triplet effective fields with $J = L - 1$, L, and $L + 1$, respectively. The four tensors are all completely symmetric and traceless and satisfy the transverse condition

$$
v_{\mu_i}K_L^{\mu_1\cdots\mu_i\cdots\mu_L} = 0, \qquad v_{\mu_j}H_J^{\mu_1\cdots\mu_j\cdots\mu_J} = 0, \tag{2}
$$

$i = 1, \ldots, L$, $j = 1, \ldots, J$. The properties of H and K under parity, charge conjugation and heavy quark spin transformations can be easily obtained by assuming that the corresponding transformation rules of the multiplet $J^{\mu_1\cdots\mu_L}$ follow as:

$$
J^{\mu_1\cdots\mu_L} \xrightarrow{P} \gamma^0 J_{\mu_1\cdots\mu_L}\gamma^0, \qquad v^\mu \xrightarrow{P} v_\mu, \tag{3a}
$$

$$
J^{\mu_1\cdots\mu_L} \xrightarrow{C} (-1)^{L+1}C[J_{\mu_1\cdots\mu_L}]^T C, \tag{3b}
$$

$$
J^{\mu_1\cdots\mu_L} \xrightarrow{S} SJ_{\mu_1\cdots\mu_L}S'^\dagger, \tag{3c}
$$

where C is the charge conjugation matrix ($C = i\gamma^2\gamma^0$ in the Dirac representation), and $S \in SU(2)_Q$ and $S' \in SU(2)_{\bar{Q}}$ correspond to the heavy quark and heavy antiquark spin-symmetry groups ($[S, \not{v}] = [S', \not{v}] = 0$).

Since we are going to consider the two-photon decay of $\psi(2S)$ into $\psi(1S)$ via the intermediate states $\chi_{cJ}(nP)$, it will be helpful to give the explicit expressions of the S- and P-wave multiplets that follow from Eq. (1). For the $L = S$ case, we have

$$
J = \frac{1+\not{v}}{2}(H_1^\mu\gamma_\mu - K_0\gamma^5)\frac{1-\not{v}}{2}, \tag{4}
$$

and for the $L = P$ case,

$$
J^\mu = \frac{1+\not{v}}{2}\Bigg\{H_2^{\mu\alpha}\gamma_\alpha + \frac{1}{\sqrt{2}}\epsilon^{\mu\alpha\beta\gamma}v_\alpha\gamma_\beta H_{1\gamma} + \frac{1}{\sqrt{3}}(\gamma^\mu - v^\mu)H_0 + K_1^\mu\gamma^5\Bigg\}\frac{1-\not{v}}{2}. \tag{5}
$$

The radiative transitions between mS and nP charmonium states in the nonrelativistic limit is given by the Lagrangian:

$$
\mathcal{L} = \sum_{m,n}\delta^{nP,mS}\text{Tr}[\bar{J}(mS)J_\mu(nP)]v_\nu F^{\mu\nu} + \text{H.c}, \tag{6}
$$

where $\delta^{nP,mS}$ is the coupling constant, and $F^{\mu\nu}$ is the electromagnetic tensor. The Lagrangian in Eq. (6) preserves parity, charge conjugation, gauge invariance, and heavy quark and antiquark spin symmetry.

Using the effective Lagrangian, it is straightforward to calculate the E1 transition decay widths:

$$
\Gamma(m^3S_1 \rightarrow n^3P_J)
$$
$$
= (2J+1)\frac{(\delta_J^{nP,mS})^2}{144\pi}k_\gamma^3\frac{(M_{mS}+M_{nP})^4}{M_{mS}^3 M_{nP}}, \tag{7a}
$$

$$
\Gamma(n^3P_J \rightarrow m^3S_1) = \frac{(\delta_J^{nP,mS})^2}{48\pi}k_\gamma^3\frac{(M_{mS}+M_{nP})^4}{M_{mS}M_{nP}^3}, \tag{7b}
$$

where k_γ is the energy of the emitted photon. The results are slightly different from those given in Refs. [40,41]. It is because the initial and final charmonium states can not be static simultaneously, and we choose different values of v_μ for them to maintain the transverse condition in Eq. (2). Namely, in the vertex (6) we have substituted the velocity v^μ in the current that produces the outgoing particle by v_f^μ, its four velocity. The remaining velocities (i.e. the explicit one and the one in the current that annihilates the incoming particle) are chosen as v_i^μ, the four velocity of the incoming particle. The explicit calculations in (7) show that these changes maintain the spin-symmetry ratios between the

TABLE I.   The numerical values of the coupling constants $\delta_J^{nP,mS}(\text{GeV}^{-1})$ are shown. For the $n = 1$ case, the results are obtained by fitting the experimental data, and for $n = 2$, the results are determined by comparing with the potential model predictions [26].

	$\chi_{c0}(1P)$	$\chi_{c1}(1P)$	$\chi_{c2}(1P)$	$\chi_{c0}(2P)$	$\chi_{c1}(2P)$	$\chi_{c2}(2P)$
J/ψ	0.211	0.230	0.228	5.27×10^{-2}	5.30×10^{-2}	5.34×10^{-2}
$\psi(2S)$	0.224	0.235	0.273	0.410	0.413	0.416

decay widths of the different states (provided that the same mass is used for each spin multiplet). Note that $v_i \cdot v_f = 1 + \mathcal{O}(v_Q^4)$, and the results of Ref. [41] differ from ours by $\mathcal{O}(v_Q^4)$ contributions. In (7) we have also allowed the coupling constant $\delta^{nP,mS}$ of the spin-symmetry multiplet to depend on the total angular momentum J, namely, $\delta^{nP,mS} \rightarrow \delta_J^{nP,mS} = \delta^{nP,mS} + \mathcal{O}(1/m^2)$. In this way we are accounting for spin-symmetry breaking terms due to the spin-orbit, spin-spin, and tensor potentials in pNRQCD (or in potential models). Note that although spin-breaking terms look like an $\mathcal{O}(1/m)$ in NRQCD (like in HQET), this is actually the case only when ultrasoft particles are emitted, for instance, in magnetic transitions, or in processes involving pseudo-Goldstone bosons [21]. Soft emissions can only be virtual and lead to the above mentioned $\mathcal{O}(1/m^2)$ spin-breaking potentials, which make the coupling constants different at this order. In conventional potential models, the differences between $\delta_J^{nP,mS}$ are usually taken to be of order v_Q^2, although on general grounds they could be as large as order v_Q [17]. $\delta^{nP,mS}$ can, in principle, be obtained by calculating the matrix element of the electromagnetic current between the wave functions of the nP and mS states in pNRQCD (or in any potential model, see Ref. [42] for a recent review). Nowadays they can also be obtained from lattice QCD [43,44]. Here we will determine their values using experimental data, except for those related to the $\chi_{cJ}(2P)$ for which experimental data is not available. In the last case the values will be estimated using a potential model.

For the $1P$ case, the $\psi(2S) \rightarrow \chi_{cJ}(1P) + \gamma$ and $\chi_{cJ}(1P) \rightarrow J/\psi + \gamma$ processes have been measured with a very high precision [45], so we can determine the values of the relevant coupling constants by comparing with the experimental results. Using the PDG data [45], $M_{2S} = 3.686$ GeV, $M_{\psi(1S)} = 3.097$ GeV, $M_{\chi_{cJ}} = 3.415$, 3.511, 3.556 GeV (for $J = 0, 1, 2$) $\Gamma_{\psi(2S)} = 304$ keV, $\Gamma_{\chi_{cJ}} = 10.3$, 0.86, 97 MeV (for $J = 0, 1, 2$), and

$$\text{Br}(\psi(2S) \rightarrow \chi_{c0} + \gamma) = 9.62\%,$$
$$\text{Br}(\chi_{c0} \rightarrow J/\psi + \gamma) = 1.16\%, \quad (8a)$$
$$\text{Br}(\psi(2S) \rightarrow \chi_{c1} + \gamma) = 9.2\%,$$
$$\text{Br}(\chi_{c1} \rightarrow J/\psi + \gamma) = 34.4\%, \quad (8b)$$
$$\text{Br}(\psi(2S) \rightarrow \chi_{c2} + \gamma) = 8.74\%,$$
$$\text{Br}(\chi_{c2} \rightarrow J/\psi + \gamma) = 19.5\%, \quad (8c)$$

we obtain the absolute values of $\delta_J^{1P,2S}$ and $\delta_J^{1P,1S}$ listed in Table I. For the $2P$ case, only the $\chi_{c2}(2P)$ [formerly called $Z(3930)$ [46]] has been included in the PDG, so we estimate the relevant parameters with the help of a potential model.

The spectrum of the $2P$ states and their radiative decay into the lower S-wave states have been calculated by numerous groups (for reviews see, e.g., Ref. [42]). By using the screened potential, the updated results of the charmonium spectrum and the E1 transition rates are given in Ref. [26]. In this work, besides setting $M_{\chi_{c2}(2P)} = 3.929$ GeV, $X(3872)$ is assigned to the $\chi_{c1}(2P)$ state and $M_{\chi_{c0}(2P)} = 3.842$ GeV is predicted. From the nonrelativistic results of $\Gamma(\chi_{cJ}(2P) \rightarrow J/\psi(\psi(2S)) + \gamma)$ presented in Table IV of Ref. [26], we obtain the absolute values of the corresponding coupling constants and give them in Table I. Because the mass differences between the $2P$ states are much smaller than the mass gap between the $2P$ and $2S$ ($1S$) states, in practice we use the center of gravity mass

$$M_{(2P)} = \frac{M_{\chi_{c0}(2P)} + 3 \times M_{\chi_{c1}(2P)} + 5 \times M_{\chi_{c2}(2P)}}{9}, \quad (9)$$

and the center of gravity coupling constant

$$\delta^{2P,ms} \equiv \frac{\delta_0^{2P,mS} + 3 \times \delta_1^{2P,mS} + 5 \times \delta_2^{2P,mS}}{9}, \quad (10)$$

rather than calculating the contribution of the individual $2P$ states.

III. DISCRETE CONTRIBUTION TO $\psi(2S) \rightarrow J/\psi + 2\gamma$

Now, we proceed to calculate the decay rate of the process $\psi(2S)(p_0) \rightarrow J/\psi(p_1) + \gamma(p_2) + \gamma(p_3)$ via intermediate states $\chi_{cJ}(nP)$. Such a $1 \rightarrow 3$ process can be described by the following dimensionless variables:

$$x_i = \frac{2p_0 \cdot p_i}{M_{\psi(2S)}^2}, \qquad \sum_i x_i = 2. \quad (11)$$

In terms of x_i, the three-body phase space $\Phi_{(3)}$ can be written as

$$d\Phi_{(3)} = \frac{M_{\psi(2S)}^2}{2(4\pi)^3} \delta(2 - x_1 - x_2 - x_3)dx_1 dx_2 dx_3. \quad (12)$$

For each intermediate $\chi_{cJ}(nP)$, there are two Feynman diagrams, which are shown in Fig. 1. The corresponding
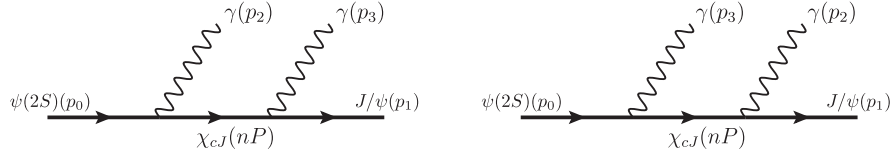
FIG. 1. The Feynman diagrams for $\psi(2S)$ decay into $J/\psi + 2\gamma$ via intermediate states $\chi_{cJ}(nP)$.

Feynman amplitude is denoted by $\mathcal{M}^{\chi_{cJ}(nP)}$. Putting the contributions of the three $2P$ states together, the total Feynman amplitude is then divided into four parts:

$$\mathcal{M}^{\text{Tot}} = \mathcal{M}^{\chi_{c0}(1P)} + \mathcal{M}^{\chi_{c1}(1P)} + \mathcal{M}^{\chi_{c2}(1P)} + \mathcal{M}^{\chi_c(2P)}. \quad (13)$$

Each of $\mathcal{M}$ on the right-hand side of the above equation can be obtained from the Lagrangian in Eq. (6) upon making the same replacements as discussed after (6). Since the propagator of the $1P$ fields may become on-shell, self-energy corrections must be considered. We approximate them by introducing a constant decay width, which, parametrically, is $\mathcal{O}(m\alpha_s^2 v_Q^5, m\alpha v_Q^4)$. Being that these figures are much smaller than mv_Q^2, $1/m$ corrections to the static propagator must be considered in order to match its size. As an alternative, we use relativistic propagators that include them. For example, the Feynman amplitude of the first diagram in Fig. 1 for $\mathcal{M}^{\chi_{c2}(1P)}$, which is the most complicated one, is

$$\mathcal{M}^{\chi_{c2}(1P)} = \delta_2^{1P,1S} \delta_2^{1P,2S} \text{Tr}\left[\frac{1 + \slashed{v}_{2s}}{2} \slashed{\epsilon}_{2s} \gamma^\alpha \frac{1 + \slashed{v}_p}{2}\right]$$

$$\times \frac{(\Pi_{\alpha\alpha_1}\Pi_{\mu\mu_1} + \Pi_{\alpha\mu_1}\Pi_{\mu\alpha_1})/2 - \Pi_{\alpha\mu}\Pi_{\alpha_1\mu_1}/3}{v_p^2 - 1 + I * \Gamma_{\chi_{c2}(1P)}/M_{\chi_{c2}(1P)}}$$

$$\times \text{Tr}\left[\frac{1 + \slashed{v}_p}{2} \gamma^{\alpha_1} \slashed{\epsilon}_{1s}^* \frac{1 + \slashed{v}_{1s}}{2}\right] v_{\nu,2S} v_{\nu,p} \bar{F}_2^{\mu\nu} \bar{F}_3^{\mu_1\nu_1}, \quad (14)$$

where $\Pi^{\alpha\beta} = (-g^{\alpha\beta} + v_p^\alpha v_p^\beta)$, $\bar{F}_i^{\alpha\beta} = p_i^\alpha \epsilon_i^{*\beta} - p_i^\beta \epsilon_i^{*\alpha}$, $v_p^\mu = (p_0^\mu - p_2^\mu)/M_{\chi_{c2}(1P)}$, and $\Gamma_{\chi_{c2}(1P)}$ is the total width of $\chi_{c2}(1P)$. In the above expression, we have omitted the imaginary unit I, which is a global factor and has no influence on the final result. For the convenience of further discussion, we also divided the decay width of the discrete part into four parts:

$$\Gamma_{\text{dis}}(\psi(2S) \to J/\psi + \gamma\gamma) = \Gamma_{\text{Ind}}^{1P} + \Gamma_{\text{Int}}^{1P} + \Gamma^{2P} \pm \Gamma_{\text{Int}}^{1,2P}, \quad (15)$$

where Γ_{Ind}^{1P} is the sum of the three individual contributions of the χ_{cJ} states, which is proportional to $\sum_{J=0}^{2} |\mathcal{M}^{\chi_{cJ}(1P)}|^2$, Γ_{Int}^{1P} is the interference between the $1P$ states $(\sim \Re\{\sum_{J \neq J'} \mathcal{M}^{*\chi_{cJ}(1P)} \mathcal{M}^{\chi_{cJ'}(1P)}\})$, Γ^{2P} is the contribution involving the $2P$ states only, and $\Gamma_{\text{Int}}^{1,2P}$ is the interference contribution between the $1P$ and $2P$ states. The "$+(-)$" sign before the last term corresponds to the two possible relative phase angles 0 (π) between the $1P$ and $2P$ states.

We have computed $\sum |\mathcal{M}^{\text{Tot}}|^2$ analytically, but the outcome is too lengthy to be presented here. After doing the phase space integrals numerically, we obtain that

$$\Gamma_{\text{Ind}}^{1P} = 15.14 \text{ keV} \simeq \sum_J \Gamma(\psi(2S) \to \gamma + \chi_{cJ})$$

$$\times \text{Br}(\chi_{cJ} \to J/\psi + \gamma),$$

$$\Gamma_{\text{Int}}^{1P} = 5.95 \times 10^{-2} \text{ keV},$$

$$\Gamma^{2P} = 2.80 \times 10^{-3} \text{ keV},$$

$$\Gamma_{\text{Int}}^{1,2P} = 4.13 \times 10^{-2} \text{ keV}. \quad (16)$$

The numerical results yield that on the total decay width level the effects of the interference among the $\chi_{cJ}(1P)$ states as well as the effect of the $2P$ states are so small that they can be neglected. We have also calculated the photon spectrum $d\Phi_{(3)}/dx_2$, and display the figures for each part separately in Figs. 2 and 3, respectively.

Since we have chosen different v for the initial and final states in Eq. (14), we may also have a nontrivial J/ψ polarization, which should be zero in the single v case. Similar to the production case [47], here, we define the polarization parameter α as

$$\alpha = \frac{\Gamma_T - 2\Gamma_L}{\Gamma_T + 2\Gamma_L}, \quad (17)$$

where Γ_T and Γ_L are the decay widths for J/ψ in the transverse and longitudinal polarization states, respectively. We calculate α in the rest frame of $\psi(2S)$ and get $\alpha \simeq -0.16$. This is slightly different from zero, and we interpret it as a purely kinematic effect. We find that α is mainly determined by the resonance contribution, being the influence of the interference and the $2P$ terms tiny.

The experimental measurement of the $\psi(2S) \to J/\psi + \gamma\gamma$ decay can be implemented in the off-mass shell region of χ_{cJ}, i.e., the experimentally sensitive region in Daltiz plot

$$0.15 < M_{\gamma\gamma} < 0.51 \text{ GeV},$$

$$3.43 < M_{J/\psi\gamma} < 3.49 \text{ GeV}, \quad (18)$$

where $M_{\gamma\gamma}$ is the invariant mass of the two photons and $M_{J/\psi\gamma}$ is the invariant mass of J/ψ and the higher energy photon. These cuts can mostly exclude the contribution from the highly yielded $\chi_{cJ}(1P)$ states. From the photon spectrum in the cut region indicated in Fig. 4, the different contributions to the decay width (15) read

$$\Gamma_{\text{Ind}}^{1P} = 4.68 \times 10^{-2} \text{ keV}, \qquad \Gamma_{\text{Int}}^{1P} = 6.5 \times 10^{-3} \text{ keV},$$

$$\Gamma^{2P} = 1.82 \times 10^{-4} \text{ keV}, \qquad \Gamma_{\text{Int}}^{1,2P} = 4.78 \times 10^{-3} \text{ keV}. \quad (19)$$
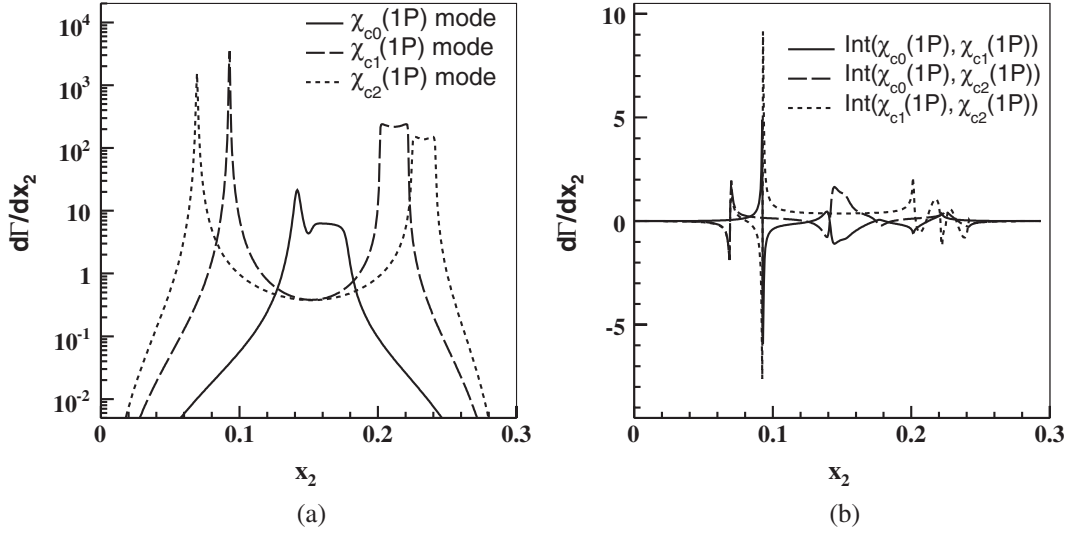
FIG. 2.   The partial decay width as a function of the photon energy fraction x_2: (a) the individual contribution of the three χ_{cJ} ($J = 0, 1, 2$) states, corresponding to $\Gamma_{\mathrm{Ind}}^{1P}$ in (15), (b) the contribution of the interference terms between the three χ_{cJ} ($J = 0, 1, 2$) states, corresponding to $\Gamma_{\mathrm{Int}}^{1P}$ in (15).
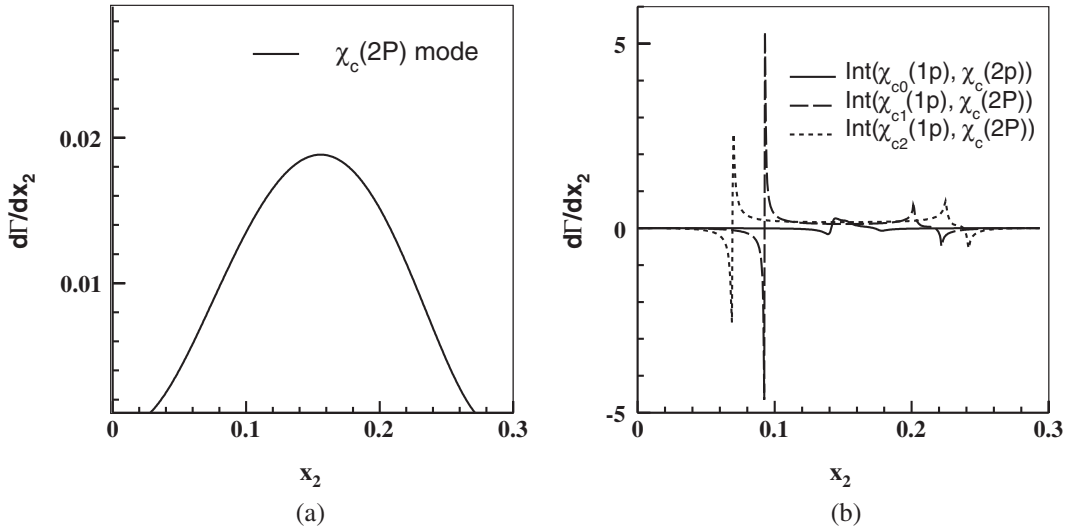

FIG. 3.   The partial decay width as a function of the photon energy fraction x_2: (a) the contribution of the $2P$ states, corresponding to Γ^{2P} in (15), (b) the contribution of the interference terms between the $2P$ and the three $1P$ states, corresponding to $\Gamma_{\mathrm{Int}}^{1,2P}$ in (15).

We have also computed the branching ratio, photon spectrum, and the polarization parameter in the cut region. The result of the branching ratio is

$$\mathcal{B}_{\mathrm{dis}}^{\mathrm{cut}}(\psi(2S) \to J/\psi + 2\gamma)$$

$$= \begin{cases} 1.92 \times 10^{-4}, & (\text{for } \theta = 0) \\ 1.60 \times 10^{-4}, & (\text{for } \theta = \pi) \end{cases}. \quad (20)$$

The result in Eqs. (19) and (20) shows that, contrary to the case of the total decay width (16), in the cut region the effect of interference among $1P$ states as well as the contribution from the $2P$ states can not be ignored. It is more than 10% of the sum of the separated contributions of

the $\chi_{cJ}(1P)$ states. The J/ψ produced in the cut region tend to be unpolarized and the polarization parameter in the cut region becomes $\alpha^{\mathrm{cut}} = -0.122$ and -0.107 for $\theta = 0$ and $\theta = \pi$, respectively. If we only include the three individual contributions of $\chi_{cJ}(1P)$, the value of α^{cut} turns to be -0.078. Finally, the different contributions to the photon spectrum in the cut region are shown in Fig. 4.

As mentioned before, the coupling constant $\delta^{nP,mS}$ is related to the spatial matrix element $\langle nP|r|mS \rangle = \int_0^\infty R_{nP}(r)R_{mS}(r)r^3 dr$ in potential models. At least three different potential models, including the Cornell potential [48] and the screened potential [26], give the phase angle θ to be π [49]. Hence, the $\theta = \pi$ option in our calculation appears to be favored.
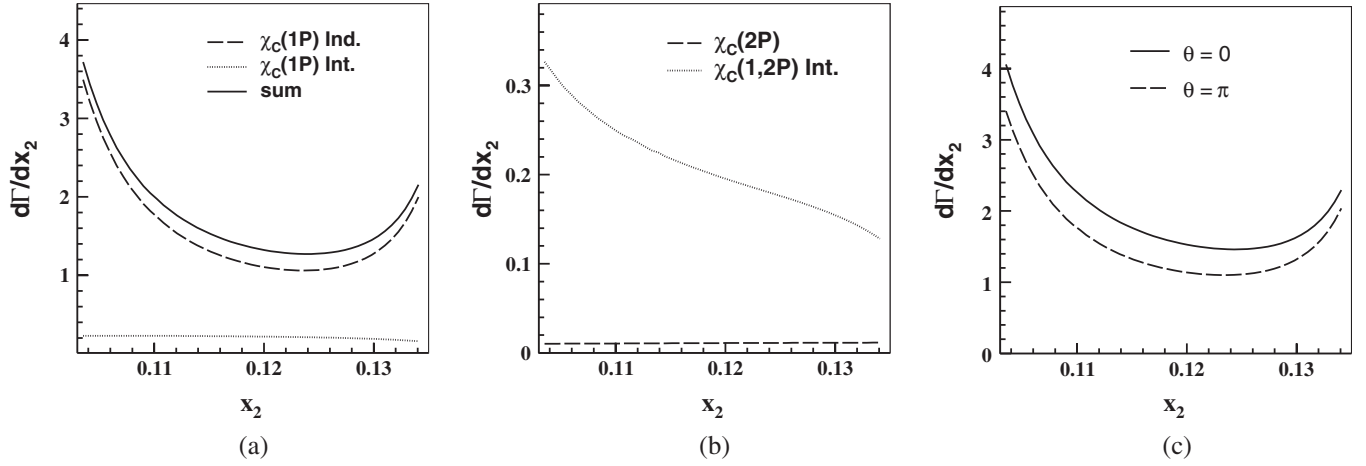
FIG. 4. The discrete contributions to the photon energy spectrum of the $\psi(2S) \to J/\psi + \gamma\gamma$ process in the cut region: (a) the contribution of the 1P states, corresponding to Γ^{1P}_{Ind} and Γ^{1P}_{Int} in (15), (b) the contribution of the 2P states and of the interference terms between 1P and 2P states, corresponding to Γ^{2P} and to $\Gamma^{1,2P}_{\text{Int}}$ in (15), (c) the total contribution for a different relative phase angle θ, corresponding to the $\pm$ sign in (15).

IV. DISCUSSION AND SUMMARY

We have estimated the discrete contribution to the $\psi(2S) \to J/\psi + \gamma\gamma$ due to electric dipole transitions in the whole phase space and, in particular, in the cut region used at BESIII. Higher multipole electric transitions and the magnetic ones are suppressed by at least v_Q^2 in the amplitude. This is also the case for contributions arising from two-photon vertices. The largest uncertainty in our calculation comes from the fact that we neglect the contribution of nP states for $n \geq 3$. This contribution is not parametrically suppressed by powers of v_Q, although we expect it to be small for the following two reasons: (i) the propagator of the nP state is increasingly off-shell when n increases, and (ii) the coupling constants $\delta_J^{nP,1S}$ and $\delta_J^{nP,2S}$ are proportional to the overlap of the radial wave functions of the corresponding states, which decreases with n. Apart from this truncation, the estimate is reliable at leading order in v_Q^2. In fact, the modifications we have made in (14), which introduce terms of higher order in v_Q, take into account relativistic effects in the kinematics, and hence help in providing a better estimate.

From the point of view of potential models, the leading corrections to the $E1$ transition processes, $\psi(2S) \to \chi_{cJ} + \gamma$ and $\chi_{cJ} \to J/\psi + \gamma$, mainly arise from the three following sources: (i) relativistic modification of the nonrelativistic wave functions, (ii) finite size effects, and (iii) contribution of high v_Q^2 order electromagnetic operators [42]. In this work, we use the effective Lagrangian, Eq. (14), to describe the $E1$ transition process. For the 1P case, we determine the values of the corresponding coupling constants from the experimental data. Thus, the effects of (i), which are dominant, are taken into account in our results, as far as the vertices involving the 1P states is concerned. Therefore, our results for the two-photon

decay width in the off-shell region are more accurate than a potential model calculation for the one-photon $E1$ transition process. Both the corrections due to (ii) and to (iii) could be taken into account by including higher dimensional operators in the vertices (6). As mentioned before these operators are suppressed by at least order v_Q^2.

Let us next discuss how our results compare with the usual inputs in the Monte Carlo (MC) codes that are used to analyze the experimental data. In the experimental treatment of the four contributions in Eq. (15) in the peaking region, usually only the first one, Γ^{1P}_{Ind}, is taken into account, and is often modeled using the nonrelativistic Breit-Wigner line shape of χ_{cJ} and J/ψ. The other three components are negligible and generally omitted. But in the off-shell region, as argued above, the other three components will be sizable and have to be considered in the data treatment. Furthermore, in the off-shell cut region (18), even this naive nonrelativistic Breit-Wigner line-shape description of the individual χ_{cJ} states contribution needs improvement. The reason is that a (single) nonrelativistic Breit-Wigner is only a good approximation to the line shape of $d\Gamma^{1P}/dx_2$ in the resonance peaking region, as shown in Fig. 2(a). In the cut region equation (18), which lies between the χ_{c0} and χ_{c1} resonance peaks, there is no guarantee that the nonrelativistic Breit-Wigners will provide a correct description of data. Let us next point out the main ingredients it misses. In the $E1$ transition process, the decay rate is proportional to the factor k_γ^3 as shown in Eq. (7). We may then improve on the nonrelativistic Breit-Wigner approximation by just introducing the correct photon energy dependence in each vertex, i.e., the full $k_{\gamma 1}^3 k_{\gamma 2}^3$ scale factor from the two $E1$ transitions. Note that if one only includes the k_γ^3 correction due to the first $E1$ transition, Γ^{1P} in the cut region will be overestimated, because the energies of the two photons are negatively correlated.
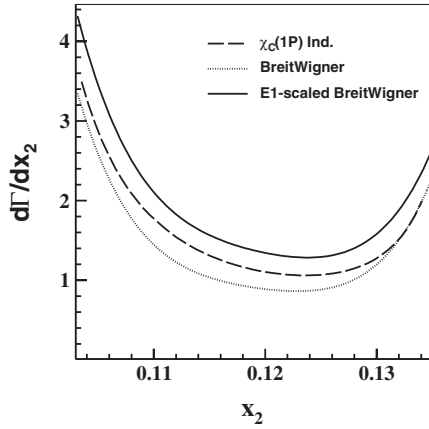
FIG. 5. The MC simulation of the cascade decay of $\psi(2S) \rightarrow (J\psi\gamma_1)_{\chi_{cJ}}\gamma_2$ in the cut region, where the branching fractions are from PDG2010 [45]. The dotted line denotes the naive non-relativistic Breit-Wigner simulation, the solid line is the simulation including the $k_{\gamma_1}^3 k_{\gamma_2}^3$ factor, and the dashed line is the contribution of the three individual $\chi_{cJ}(1P)$ states, corresponding to $\Gamma_{\mathrm{Ind}}^{1P}$ in (15), calculated in this paper.

In Fig. 5, the MC simulation results of the line shapes in the cut region are shown, which are implemented in two ways. One is done by including the $k_{\gamma_1}^3 k_{\gamma_2}^3$ correction from a double $E1$ transition, and the other one is not. The difference between these two MC simulation results can be understood as follows: the $E1$ transition enhances the right tail of photon energy peak and depresses the left tail of the nonrelativistic Breit-Wigner. As a whole, the effect of the correlated emitted photons in the double $E1$ transition increases the χ_{cJ} contribution in the cut region. For comparison, we also plot the effective Lagrangian result of the sum of the three individual χ_{cJ} states contribution in Fig. 5. It is clear that neither of the simulation results agree with that of the effective Lagrangian calculation, although they are qualitatively similar. From the amplitude in Eq. (14), it can be verified that the $k_{\gamma_1}^3 k_{\gamma_2}^3$ factor and the

nonrelativistic Breit-Wigner is only the leading-order non-relativistic approximation of the effective Lagrangian calculation in the off-shell region. Hence, even for a delicate description of the individual contribution in the off-shell region, including the double $E1$ transition correction in the naive nonrelativistic Breit-Wigner only may not be enough.

In summary, we have estimated the discrete contribution to the $\psi(2S) \rightarrow J/\psi + \gamma\gamma$ due to electric dipole transitions in the whole phase space and, in particular, in the cut region in the experimental measurement. We find that for the full decay width the interference contribution and the contributions of higher excited states can be safely neglected. However, in the regions of the phase space off the resonance peaks, their contributions are considerable and important for a delicate experimental measurement. As argued in the Introduction, a large deviation of our results from an experimental observation would indicate that the effects of the $D\bar{D}$ threshold are significant.

ACKNOWLEDGMENTS

[1] E. S. Swanson, Phys. Rep. **429**, 243 (2006).
[2] S. L. Zhu, Int. J. Mod. Phys. E **17**, 283 (2008).
[3] M. Nielsen, F. S. Navarra, and S. H. Lee, Phys. Rep. **497**, 41 (2010).
[4] N. Brambilla *et al.*, Eur. Phys. J. C **71**, 1534 (2011).
[5] E. Eichten, K. Gottfried, T. Kinoshita, K. D. Lane, and T. M. Yan, Phys. Rev. D **17**, 3090 (1978); **21**, 313(E) (1980).
[6] E. Eichten, K. Gottfried, T. Kinoshita, K. D. Lane, and T. M. Yan, Phys. Rev. D **21**, 203 (1980).
[7] K. Heikkila, S. Ono, and N. A. Tornqvist, Phys. Rev. D **29**, 110 (1984); **29**, 2136(E) (1984).
[8] G. Bali and C. Ehmann, Proc. Sci. LAT2009 (2009) 113.

[9] G. S. Bali, H. Neff, T. Duessel, T. Lippert, and K. Schilling (SESAM Collaboration), Phys. Rev. D **71**, 114513 (2005).
[10] C. Downum, in *IX International Conference on Quark Confinement and Hadron Spectrum: QCHS-09*, AIP Conf. Proc. No. 1343 (AIP, New York, 2010).
[11] W. E. Caswell and G. P. Lepage, Phys. Lett. **167B**, 437 (1986).
[12] B. A. Thacker and G. P. Lepage, Phys. Rev. D **43**, 196 (1991).
[13] G. T. Bodwin, E. Braaten, and G. P. Lepage, Phys. Rev. D **51**, 1125 (1995); **55**, 5853(E) (1997).
[14] M. Neubert, Phys. Rep. **245**, 259 (1994).

[15] N. Brambilla, A. Pineda, J. Soto, and A. Vairo, Nucl. Phys. **B566**, 275 (2000).

[16] N. Brambilla, A. Pineda, J. Soto, and A. Vairo, Phys. Rev. D **63**, 014023 (2000).

[17] A. Pineda and A. Vairo, Phys. Rev. D **63**, 054007 (2001); **64**, 039902(E) (2001).

[18] N. Brambilla, A. Pineda, J. Soto, and A. Vairo, Phys. Lett. B **580**, 60 (2004).

[19] N. Brambilla, A. Pineda, J. Soto, and A. Vairo, Rev. Mod. Phys. **77**, 1423 (2005).

[20] P. Artoisenet, E. Braaten, and D. Kang, Phys. Rev. D **82**, 014013 (2010).

[21] F. K. Guo, C. Hanhart, G. Li, U. G. Meissner, and Q. Zhao, Phys. Rev. D **83**, 034013 (2011).

[22] T. Barnes and E. S. Swanson, Phys. Rev. C **77**, 055206 (2008).

[23] A. Le Yaouanc, L. Oliver, O. Pene, and J. C. Raynal, Phys. Rev. D **8**, 2223 (1973).

[24] T. Barnes, AIP Conf. Proc. **1257**, 11 (2010).

[25] K. J. Sebastian, Phys. Rev. D **26**, 2295 (1982).

[26] B. Q. Li and K. T. Chao, Phys. Rev. D **79**, 094004 (2009).

[27] E. J. Eichten, K. Lane, and C. Quigg, Phys. Rev. D **69**, 094019 (2004).

[28] D. Guetta and P. Singer, Phys. Rev. D **61**, 054014 (2000).

[29] C. J. Biddick *et al.*, Phys. Rev. Lett. **38**, 1324 (1977); W. Bartel *et al.*, Phys. Lett. **79B**, 492 (1978); R. Brandelik *et al.* (DASP Collaboration), Nucl. Phys. **B160**, 426 (1979).

[30] T. Himel *et al.*, Phys. Rev. Lett. **44**, 920 (1980); M. Oreglia *et al.*, Phys. Rev. Lett. **45**, 959 (1980); Phys. Rev. D **25**, 2259 (1982); J. Gaiser *et al.*, Phys. Rev. D **34**, 711 (1986).

[31] J. Z. Bai *et al.* (BES Collaboration), Phys. Rev. D **70**, 012006 (2004).

[32] M. Ablikim *et al.* (BES Collaboration), Phys. Rev. D **71**, 092002 (2005).

[33] N. E. Adam *et al.* (CLEO Collaboration), Phys. Rev. Lett. **94**, 232002 (2005).

[34] H. Mendez *et al.* (CLEO Collaboration), Phys. Rev. D **78**, 011102 (2008).

[35] F. A. Harris (BESIII Collaboration), Int. J. Mod. Phys. A **26**, 347 (2011).

[36] N. Brambilla, D. Eiras, A. Pineda, J. Soto, and A. Vairo, Phys. Rev. Lett. **88**, 012003 (2001).

[37] A. A. Penin, A. Pineda, V. A. Smirnov, and M. Steinhauser, Nucl. Phys. **B699**, 183 (2004); **B829**, 398 (E) (2010).

[38] N. Brambilla, Y. Jia, and A. Vairo, Phys. Rev. D **73**, 054005 (2006).

[39] Y. Kiyo, A. Pineda, and A. Signer, Nucl. Phys. **B841**, 231 (2010).

[40] R. Casalbuoni, A. Deandrea, N. Di Bartolomeo, R. Gatto, F. Feruglio, and G. Nardulli, Phys. Lett. B **302**, 95 (1993).

[41] F. De Fazio, Phys. Rev. D **79**, 054015 (2009).

[42] E. Eichten, S. Godfrey, H. Mahlke, and J. L. Rosner, Rev. Mod. Phys. **80**, 1161 (2008).

[43] J. J. Dudek, R. G. Edwards, and D. G. Richards, Phys. Rev. D **73**, 074507 (2006).

[44] J. J. Dudek, R. Edwards, and C. E. Thomas, Phys. Rev. D **79**, 094504 (2009).

[45] K. Nakamura *et al.* (Particle Data Group), J. Phys. G **37**, 075021 (2010).

[46] S. Uehara *et al.* (Belle Collaboration), Phys. Rev. Lett. **96**, 082003 (2006).

[47] B. Gong and J. X. Wang, Phys. Rev. Lett. **100**, 232001 (2008).

[48] E. Eichten, K. Gottfried, T. Kinoshita, J. B. Kogut, K. D. Lane, and T. M. Yan, Phys. Rev. Lett. **34**, 369 (1975); **36**, 1276(E) (1976).

[49] Bai-Qing Li, (private communication).